Journal of Inorganic Biochemistry 103 (2009) 43–49

Contents lists available at ScienceDirect

Journal of Inorganic Biochemistry

journal homepage: www.elsevier.com/locate/jinorgbio

Carbon nanotube-enhanced DNA biosensor for DNA hybridization detection using manganese(II)–Schiff base complex as hybridization indicator

Shuyan Niu, Min Zhao, Rui Ren, Shusheng Zhang *

Key Lab of Eco-chemical Engineering, Ministry of Education, College of Chemistry and Molecular Engineering, Qingdao University of Science and Technology, Qingdao 266042, PR China

ARTICLE INFO

Article history:
Received 23 April 2008
Received in revised form 9 September 2008
Accepted 9 September 2008
Available online 18 September 2008

Keywords:
Carbon nanotubes
Differential pulse voltammetry
Schiff base
Hybridization
Electrochemical DNA biosensor

ABSTRACT

A Mn(II) complex, MnL (L = sodium (*E*)-3-((1-carboxyethylimino)methyl)-4-hydroxybenzenesulfonate), was synthesized and characterized using elemental analysis and IR spectroscopy. Cyclic voltammetry (CV) and fluorescence spectroscopy were used to investigate the interaction between MnL and salmon sperm DNA. It was revealed that MnL presented high electrochemical activity on glassy carbon electrode (GCE), and it could be intercalated into the double helices of double-stranded DNA (dsDNA). Using MnL as the hybridization indicator, a novel and sensitive electrochemical DNA biosensor based on multiwall carbon nanotubes functionalized with carboxyl groups (MWCNTs–COOH, on which DNA probes were covalently immobilized) was prepared. The target single-stranded DNA (ssDNA) could be quantified ranging from 6.7×10^{-10} M to 8.4×10^{-9} M with good linearity ($r = 0.9922$). A detection limit of 1.4×10^{-10} M (3σ, $n = 9$) was achieved.

1. Introduction

Over the past decades, DNA sensing has become increasingly important, particularly with the advances in genetics, pathology, criminology, pharmacogenetics, food safety and many other fields. Because of its intrinsic specificity, the hybridization between complementary single-stranded DNA (ssDNA) chains has been used as a bio-recognition event in the design of a great number of DNA biosensors. This recognition event has been utilized through various ways, such as optical, mechanical or electrochemical [1,2]. Electrochemical DNA biosensors are attractive devices for their abilities of converting DNA hybridization event into an analytical electronic signal to obtain sequence-specific information, and are applied in clinical, environmental or forensic investigations [3].

Immobilization of DNA probes on an electrode surface has been the focus of the study on electrochemical DNA biosensors. Several methods have been used to anchor DNA strands, such as adsorption, direct covalent binding [4], entrapment in a polymer matrix [5] or indirect binding of biotin-modified DNA probe through intermediate systems such as avidin or streptavidin-modified matrix [6]. Recently, the modification of electrochemical sensors with carbon nanotubes (CNTs) has attracted considerable attention in the field of DNA sensing technology, because such modification can drastically improve the effective surface area of the electrodes, and CNTs are rather chemically stable and well conductive, so that CNTs-modified electrodes always show high performance in electrochemical analysis, especially high sensitivity. Thus, many different schemes for electrochemical DNA sensing based on CNTs have been reported [7–11].

The binding mechanisms between DNA and various redox substances, such as metal complexes [12,13], anticancer or antivirus drugs [14] and organic dyes [15,16], have been extensively investigated. For example, the binding of DNA with chelate complexes, formed by Fe(II), Ru(II) [17], Os(II/III) [18] with 1,10-phenanthroline or 2,2′-bipyridine, have been studied voltammetrically. The hybridization indicators, which are compounds that interact in measurably different ways with ssDNA and with dsDNA, are thus developed and are often employed in the detection of DNA hybridization. Numerous DNA hybridization indicators based on Os(II/III) and Ru(II) complexes have been reported due to their high sensitivity and selectivity [19,20], but compounds containing Os(II/III) and Ru(II) are usually expensive and highly poisonous, so that they are not convenient for practical applications. On the contrary, Mn(II) complexes are much cheaper and less harmful, but little Mn(II) complexes have been used as DNA intercalator. In our laboratory, many efforts were also conducted to explore the interaction between metal complexes and DNA [21–23]. It has been found that the coordination geometries and the donor atoms of the ligands play key roles in determining the binding mode between metal complexes and DNA. On the other hand, the metal ions and their flexible valences, which are responsible for the geometry of complexes, affect the intercalating ability of metal complexes to DNA [24].

* Corresponding author. Tel./fax: +86 532 84022750.
E-mail address: shushzhang@126.com (S. Zhang).

0162-0134/$ - see front matter © 2008 Elsevier Inc. All rights reserved.
doi:10.1016/j.jinorgbio.2008.09.001

In this work, carboxyl-functionalized multiwall carbon nanotubes (MWCNTs–COOH) and Mn(II)–Schiff base complex intercalators were utilized in the fabrication of DNA electrochemical biosensor. The presence of carboxyl groups on carbon nanotubes is necessary for the covalent bonding of the oligonucleotides. Oligonucleotide probes with an amino group at the 5′-phosphate end can form covalent bonds with the carboxyl groups in MWCNTs–COOH with the aid of 1-ethyl-3-(3-dimethylaminopropyl)carbodiimide (EDC). A Schiff base complex, MnL (L = sodium (*E*)-3-((1-carboxyethylimino)methyl)-4-hydroxybenzenesulfonate) was synthesized, characterized and used as the indicator for the detection of hybridization between the probe DNA and the target sequence. This sensor and the related procedure would be of lower cost and more convenience compared with many DNA sensors developed in the past decade [25–27] while still possess relatively high selectivity and sensitivity.

2. Experiment

2.1. Apparatus

The IR spectra were recorded on a Nicolet 510P FT-IR spectrometer (Nicolet, USA) in the wavenumber range of 400–4000 cm^{-1} using KBr sheets. Elemental analysis (EA) was performed on Elementar vario EL III analyzer**.** All electrochemical measurements, including cyclic voltammetry (CV), differential pulse voltammetry (DPV) and electrochemical impedance spectroscopy (EIS) were carried out with Model CHI 832B and CHI 660C electrochemical analyzers (CH Instruments, USA). A three-electrode system was employed, including Pt wire as the auxiliary electrode, Ag/AgCl as the reference electrode and glassy carbon electrode (GCE) as the working electrode. Scanning electron microscope (SEM) images were acquired with JSM-6700F cold field emission scanning electron microscope (Japan). Spectroscopic experiments were conducted on Hitachi F-4500 fluorescence spectrometer (Japan).

2.2. Reagents

Salmon sperm DNA (dsDNA) was purchased from Shanghai Huashun Biological Engineering Company ($\geqslant$95%, $A_{260}/A_{280} > 1.8$, $\varepsilon_{260} = 6600\ M^{-1}\ cm^{-1}$). Ethidium bromide was also purchased from Shanghai Huashun Biological Engineering Company and was dissolved to the desired concentration in ultrapure water (10 mg mL^{-1}). EDC was purchased from Sigma and used without further purification. MWCNTs with a diameter of about 10–30 nm and a length of around 1–10 μm were obtained from Sun Nanotech Co. Ltd. (Jiangxi, China).

Three 24-base oligonucleotides were purchased from SBS Genetech Company (Beijing, China), and purified using polyacrylamide gel electrophoresis (PAGE) to obtain the purity of $\geqslant$95.0%. The base sequences were as follows:

ssDNA probe (S_1): 5′-NH_2-GAG CGG CGC AAC ATT TCA GGT CGA-3′; Complementary target ssDNA (S_2): 5′-TCG ACC TGA AAT GTT GCG CCG CTC-3′.
Three-base mismatch target ssDNA (S_3): 5′-TCG *T*CC TGA AA*C* GTT GCG C*CT* CTC-3′.
Single mismatch target ssDNA (S_4): 5′-TCG ACC TGA AA*C* GTT GCG CCG CTC-3′.
The italicized bases in S_3 and S_4 indicate those mismatched with S_1.

All oligonucleotide stock solutions were prepared in TE solution (10 mM Tris–HCl plus 1 mM EDTA, at pH 8.0). Other chemicals employed were all of analytical grade. Ultrapure water was used throughout.

2.3. Preparation of MnL

The complex MnL (Scheme 1) was synthesized as follows [28,29]: 0.0800 g (2 mmol) NaOH, 1 mmol DL-alanine and 1 mmol sodium 3-formyl-4-hydroxybenzenesulfonate were dissolved in 10 mL 85% ethanol. Manganese(II) chloride (1 mmol) in 2.0 mL water was added dropwise to the mixture, which was refluxed for 2 h with continuous stirring. It was allowed to cool at room temperature and a brown precipitate was filtered, washed with anhydrous ethanol, and MnL was obtained as product after vacuum drying for 24 h.

Elemental analysis: Calcd. (for MnL): C, 32.79; H, 2.73; N, 3.83. Found: C, 32.32; H, 2.97; N, 3.53%. IR (cm^{-1}, w, weak; s, strong; vs, very strong): 3405vs (–OH), 1636s (C=N), 1474w (carbon backbone in phenyl), 1574s, 1387w ($-COO^-$), 1190w, 1124w (C–O bond in $-COO^-$), 1210w, 1047w (O–Ph), 1024s, 678w (C—SO_3^-), 463w (Mn–N).

2.4. Electrochemical behavior of the interaction between MnL and dsDNA

The glassy carbon electrode (GCE) was polished successively with 1.0 μm, 0.3 μm and 0.05 μm α-Al_2O_3 suspension, followed with extensively rinse in ultrapure water with sonication. Appropriate amount of dsDNA and MnL was mixed and incubated in 0.2 M NaOAc–HOAc buffer (pH 6.0) for 15 min. The interaction between MnL and dsDNA was characterized using cyclic voltammetric method in the potential scan range from 1.0 V to 0 V at the scan rate of 0.1 V s^{-1}. The fluorescence analysis was performed using ethidium bromide as indicator. The dependence between ionic strength and the CV response was investigated by applying different concentration of NaCl on the dsDNA/MnL system.

2.5. ssDNA covalently immobilized to the MWCNTs–COOH modified GCE surface

MWCNTs–COOH was prepared by mixing the commercially available MWCNTs in concentrated nitric acid for 10 h. They were then suspended in DMF under sonication to obtain MWCNTs–COOH suspension.

The covalent immobilization of oligonucleotides to MWCNTs–COOH on GCE was conducted as follows: 10 μL of 1 mg mL^{-1} suspension of MWCNTs–COOH was dropped onto a freshly smoothed GCE surface uniformly, and the solvent was then evaporated under an infrared lamp. The electrode was thoroughly rinsed, first with ethanol, and then with ultrapure water to remove excessive nanotubes. For oligonucleotide immobilization, the MWCNTs–COOH

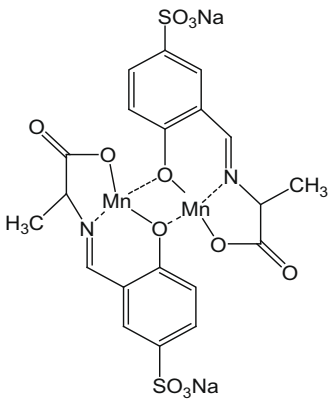

Scheme 1. Formula of MnL (L = sodium (*E*)-3-((1-carboxyethylimino)methyl)-4-hydroxybenzenesulfonate).

modified electrode was immersed in a 30 mM acetate buffer (pH 5.2) containing 10 mM EDC for 1 h. The EDC-attached electrode was washed with acetate buffer and subsequently incubated in a 3.5 μM oligonucleotides/acetate buffer solution for 12 h at room temperature to allow the probe oligonucleotides to be immobilized on the MWCNTs through the covalent amide bonds formed by the carboxyl groups on the nanotubes and the amino groups on the oligonucleotides. Scanning electron microscope (SEM) was employed to demonstrate the difference between the bare GCE (Fig. 1a) and the MWCNTs–COOH modified GCE (Fig. 1b).

2.6. Hybridization on the ssDNA-immobilized electrode

The hybridization was carried out on S_1-immobilized electrode in 0.20 M NaOAc–HOAc buffer solution (pH 6.0) containing complementary ssDNA segment (S_2), three-base mismatch ssDNA segment (S_3) or single mismatched ssDNA (S_4). The solution was stirred for 1 h at 40 °C, and then the electrode was dried at room temperature, and rinsed with 0.20 M NaOAc–HOAc buffer and ultrapure water successively to remove extra target ssDNA.

2.7. Binding of hybridization indicator

The binding of MnL on the ssDNA-immobilized or dsDNA-immobilized electrode was performed as follows: The electrode was immersed in 0.20 M NaOAc–HOAc buffer (pH 6.0) containing 5.0×10^{-5} M MnL for 15 min at room temperature, and then rinsed with ultrapure water to remove the extra MnL.

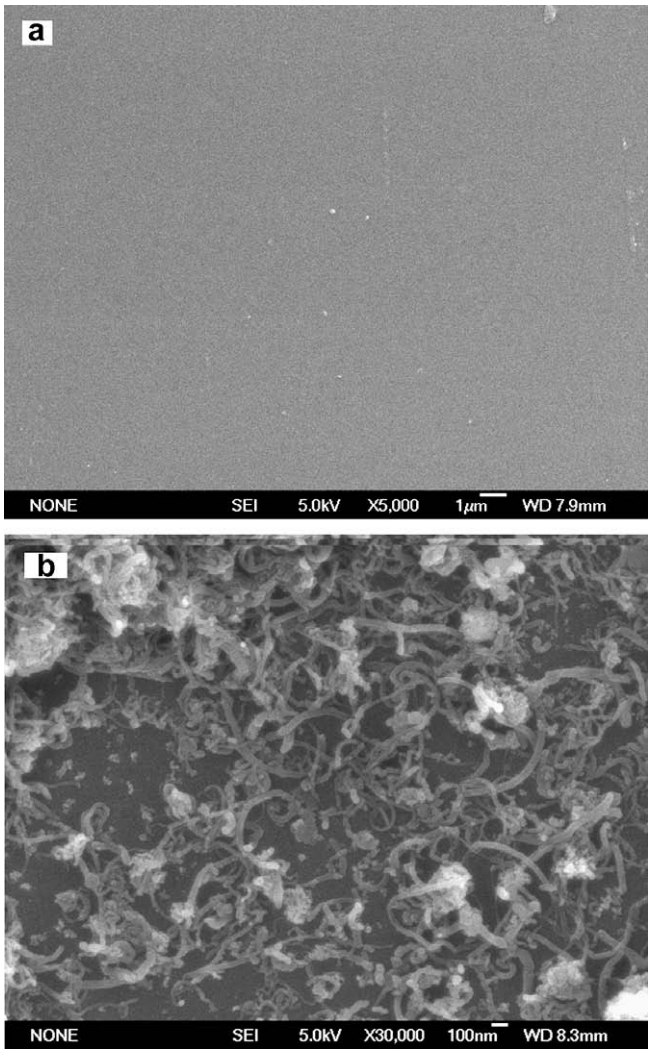

Fig. 1. SEM image glassy carbon electrode: (a) bare GCE; (b) MWCNTs–COOH modified GCE.

2.8. Electrochemical detection of target DNA sequence

The electrochemical investigation of hybridization was carried out using DPV measurements in 0.20 M NaOAc–HOAc buffer solution (pH 6.0), in a potential scanning range from 1.0 V to 0 V. The peak current related to the reduction of MnL at approximately 0.50 V was adopted as the detection signal.

The procedure of the preparation and operation of the sensor, including the modification of MWCNTs–COOH, immobilization, hybridization and detection of DNA, was illustrated in Scheme 2.

3. Results and discussion

3.1. Interaction between MnL and dsDNA

3.1.1. CV study of the interaction between dsDNA and MnL

CV was employed to explore the interaction between MnL and dsDNA. Cyclic voltammograms (Fig. 2) were obtained at 25 °C on bare GCE, in a 0.20 M pH 6.0 NaOAc–HOAc buffer containing 1.0×10^{-4} M MnL, without dsDNA (curve 1) and containing dsDNA of various concentrations (curve 2–4), respectively. A couple of non-reversible redox peaks for MnL were observed at 415 mV vs Ag/AgCl in cathodic process and 678 mV vs Ag/AgCl in anodic process in the absence of dsDNA. The formal potentials shifted in positive direction after dsDNA of different concentrations were added, and it was shown that the potential shifts increased with the dsDNA concentration, and the largest shifts (415–469 mV and 678–742 mV) were observed, when dsDNA reached a concentration of 1×10^{-3} M. This demonstrated that the interaction between MnL and dsDNA occurred. The decrease of peak current could be attributed to the accumulation of the MnL on the electrode surface as a result of the interaction between the dsDNA helices and the planar ring systems in MnL. The electrochemically active metal centers of MnL were enveloped by the bulky dsDNA molecule on the GCE surface, thus signal of MnL was reduced [30]. It has been well demonstrated by Pang and Abruna [31] that the binding mode between dsDNA and small molecules would be electrostatic interaction if the formal potential shifted negatively after the addition of dsDNA, and intercalated interaction for the positively shifted formal potential. So in our studied system, the binding mode between MnL and dsDNA could be simply attributed to the intercalated interaction. When the concentration of dsDNA was fixed, the cathodic peak current (I_{pc}) decreased linearly with the increase of concentration of MnL (plotted as $\lg[\Delta I_{pc}/\Delta I_{pc,max} - \Delta I_{pc}]$ to lg[MnL] in (Fig. 3). The binding constant between MnL and salmon sperm dsDNA was calculated to be 6.03×10^{20} $(M)^{-3}$ with a correlation coefficient of 0.9885.

3.1.2. Optimization of experimental parameters

The influence of experimental conditions, including the pH of NaOAc–HOAc buffer and the reaction time, were explored for optimum analytical performance. pH 6.0 was adopted because the maximum peak current change (before and after addition of dsDNA) was obtained. After incubation of 15 min the peak current reached a constant value, therefore, 15 min was chosen as the reaction time. The cyclic voltammograms of bare GCE in NaOAc–HOAc buffer (pH 6.0) containing 1.0×10^{-4} M MnL at different scan rates were shown in Fig. 4. The cathodic peak current of MnL increased with the increasing of scan rate. A linear relationship between the cathodic peak currents and the square roots of scan rates in the range from 20 mV s^{-1} to 150 mV s^{-1} was observed (as shown in

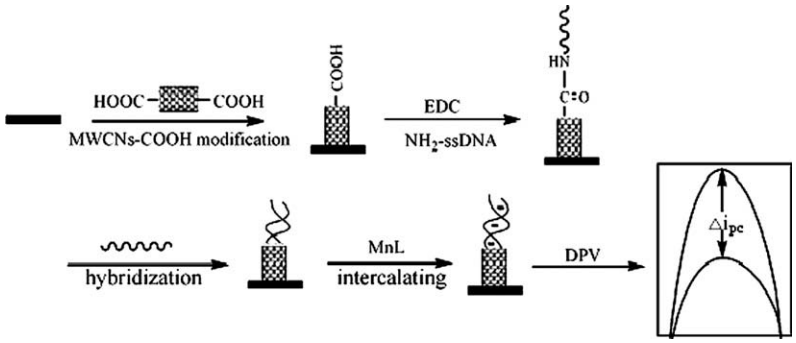

Scheme 2. Procedure for the preparation of MWCNT-modified GCE and immobolization and detection of DNA.

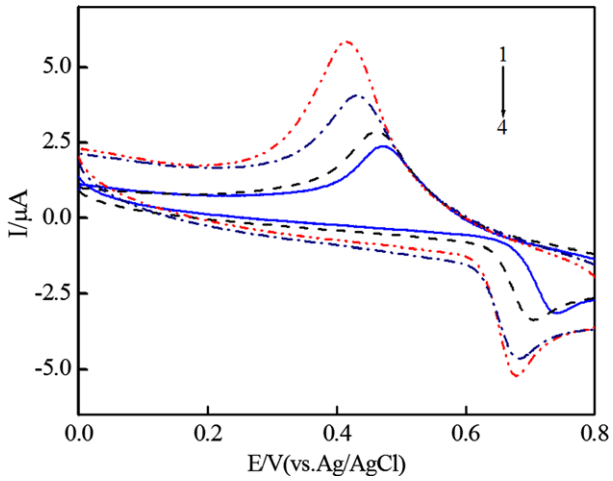

Fig. 2. Cyclic voltammograms of MnL in the absence and presence of dsDNA: (1) 1.0×10^{-4} M MnL; (2) 1.0×10^{-4} M MnL and 1.0×10^{-6} M dsDNA; (3) 1.0×10^{-4} M MnL and 1.0×10^{-4} M dsDNA; (4) 1.0×10^{-4} M MnL and 1.0×10^{-3} M dsDNA.

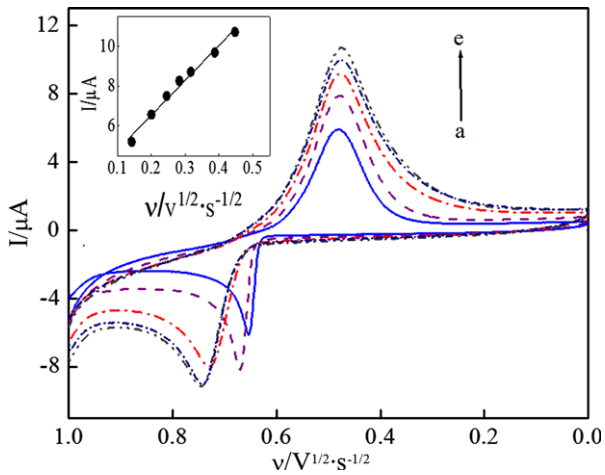

Fig. 4. Cyclic voltammograms on bare GCE in NaOAc–HOAc buffer (pH 6.0) containing 0.1 mM MnL at different scan rates: (a) 20 mV s^{-1}; (b) 60 mV s^{-1}; (c) 80 mV s^{-1}; (d) 100 mV s^{-1}; (e) 120 mV s^{-1}.

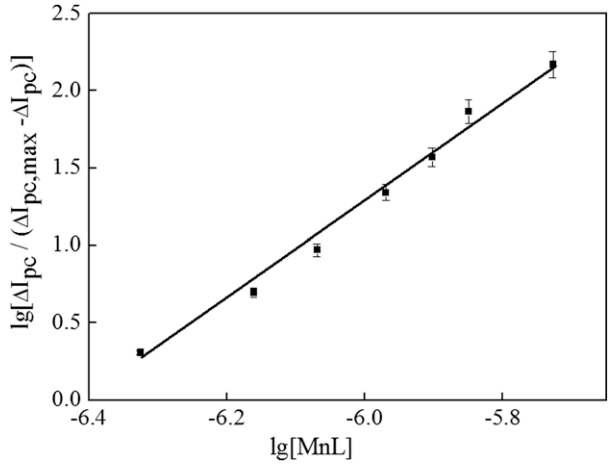

Fig. 3. The relationship between ΔI_{pc} and [MnL] in the CV investigation of MnL–dsDNA intercalation.

the inset of Fig. 4), indicating that the electro-reduction process of MnL was diffusion-controlled.

3.1.3. Ionic strength dependencies of the interaction between dsDNA and MnL

Ionic strength dependence of the interaction between dsDNA and MnL was also investigated to confirm the binding mode between MnL and dsDNA. As is well known, when the ionic strength of the solution was increased by adding salt, there would be a charge compensation to the nucleotide phosphates by cations, which would in turn hinder the electrostatic binding [19]. In this case, if the binding mode between MnL and dsDNA were predominantly electrostatic, the manganese(II) complex bound to dsDNA would be partially replaced by the sodium ions when the concentration of NaCl increased. Thus, an increased peak current of MnL should be incurred by the increase of free MnL in the solution followed with the increase of solution ionic strength. On the contrary, none or virtually small peak current change could be attributed to the case of intercalating mode. In the experiment, neither significant change in peak current nor peak potential was observed when concentration of NaCl in the solution varied from 0.015 M to 0.20 M. Thus, the interaction between dsDNA and MnL was mainly intercalative mode. The NaCl concentration for target ssDNA detection was then set as 0.10 M.

3.1.4. Fluorescence spectroscopic study of the interaction between MnL and dsDNA

The fluorescence spectra (Fig. 5) of EB–dsDNA system containing different amounts of MnL were also performed to confirm the intercalative binding mode between MnL complex and dsDNA. Significant increase of fluorescence intensity was observed after adding dsDNA to EB solution (curve a and e), since the EB molecules could be intercalated into the double helices of dsDNA molecule. The quenching of fluorescence of EB was observed, when different amounts of MnL were added in EB–dsDNA system (curve b, c and

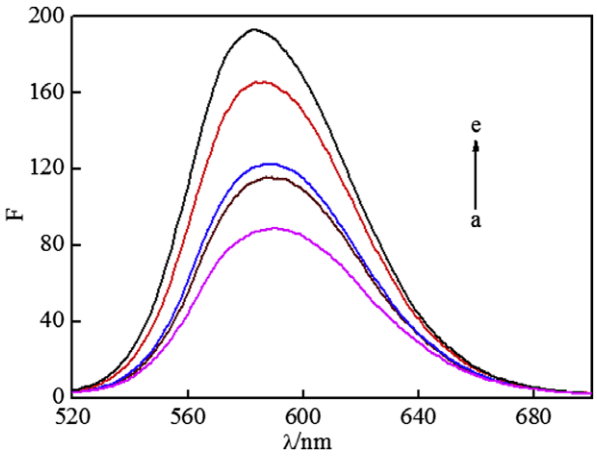

Fig. 5. Fluorescence spectra of EB–DNA system in the absence and presence of MnL. E_x = 370 nm; C_{dsDNA}: 0.34 mM; C_{EB}: 3.4×10^{-2} mM: (a) EB; (b) EB + dsDNA + 0.12 mM MnL; (c) EB + dsDNA + 8.0×10^{-2} mM MnL; (d) EB + dsDNA + 4.3×10^{-2} mM MnL; (e) EB + dsDNA.

d). It was thus deduced that the intercalated EB molecules on dsDNA could be replaced partially or fully by MnL, which accounted for the decrease of fluorescence intensity. Thus, it could be concluded that the binding of MnL with dsDNA was conducted mainly in the intercalation mode.

3.2. Electrochemical characteristics of oligonucleotides/MWCNT-COOH/GCE

CV was employed to characterize oligonucleotides/MWCNTs–COOH/GCE from −0.40 V to +1.0 V. The electrochemical responses of bare GCE (curve a), MWCNTs–COOH/GCE (curve b) and oligonucleotides/MWCNT-COOH/ GCE (curve c) in 0.1 M PBS (pH 7.0) were shown in Fig. 6. It was demonstrated that after MWCNTs–COOH was deposited on GCE, a pair of stable redox peaks appeared at −0.05 V and 0.0 V, which were attributed to the reduction and oxidation of carboxyl on MWCNTs–COOH, respectively [32]. Compared with the bare GCE, the background current of the MWCNTs–COOH/GCE was apparently large; showing that modification of the electrode with MWCNTs–COOH could significantly enlarge the effective electrode surface area as well as provide effective binding groups for oligonucleotides. As a result of the coupling of oligonucleotide probes to MWCNTs–COOH/GCE, the CV current of the electrode decreased significantly.

3.3. ssDNA hybridization detection using impedance spectroscopy

EIS was applied to monitor the whole procedure in the modification of the electrode. A typical EIS curve includes a semicircular part and a linear part. The semicircular part, obtained at higher frequency, corresponds to the electron-transfer-limited process and its diameter is equal to the electron-transfer resistance (R_{et}), which controls the electron-transfer kinetics of the redox-probe on the electrode interface; the linear part, obtained at lower frequency, corresponds to the diffusion process. $Fe(CN_6)^{3-/4-}$ was chosen as the EIS probe. The EIS curves of the MWCNTs–COOH/GCE (curve a), ssDNA/MWCNTs–COOH/GCE (curve b) and S_1–S_2 hybridized/MWCNTs–COOH/GCE (curve c) were shown in Fig. 7, obtained in a solution of 0.10 M KCl containing 10 mM $Fe(CN_6)^{3-/4-}$. When ssDNA was modified on the MWCNTs–COOH/GCE, the diameter of semicircular part greatly increased, suggesting the electron-transfer of the redox-probe was obstructed by ssDNA. The highest electron-transfer resistance, illustrated by the diameter of semicircular part in the EIS curve of S_1–S_2 hybridized/MWCNTs–COOH/GCE, was attributed to the low conductivity of dsDNA double helices structure, which slowed down the redox reaction of $Fe(CN_6)^{3-/4-}$. It was thus testified that ssDNA was immobilized on the GCE surface, and target ssDNA was hybridized with the probe ssDNA.

3.4. The selectivity of the prepared electrochemical DNA biosensor

The MnL complex was used as DNA hybridization indicator for the detection of a 24-mer oligonucleotide which is specific for colitoxin, and the selectivity of this assay was investigated. The DPV curves obtained in 0.20 M NaOAc–HOAc buffer (pH 6.0) were shown in Fig. 8, on MWCNTs–COOH/GCE with probe ssDNA (S_1) immobilized (curve a), after the hybridization of S_1 and complementary ssDNA (S_2) (curve d and e), after the applying of three-base mismatch target ssDNA (S_3) (curve b) and after the applying of single mismatched target ssDNA (S_4) (curve c), respectively. Each measurement was performed after MnL was sufficiently accumulated, and was repeated on at least three GCEs, and the mean value of the three closest readouts was adopted as the measurement result. It was found that there was only a small DPV peak response of MnL for S_1 modified MWCNTs–COOH/GCE (curve a),

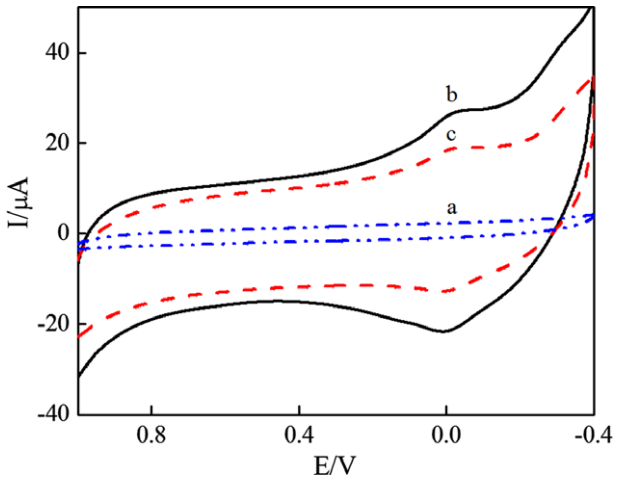

Fig. 6. Cyclic voltammograms of bare GCE (curve a), MWCNTs–COOH/GCE (curve b) and oligonucleotide/MWCNTs–COOH/GCE (curve c) recorded in 0.1 M PBS blank solution (pH 7.0). Scan rate 0.10 V s^{-1}; scan range +1.0 V to −0.40 V.

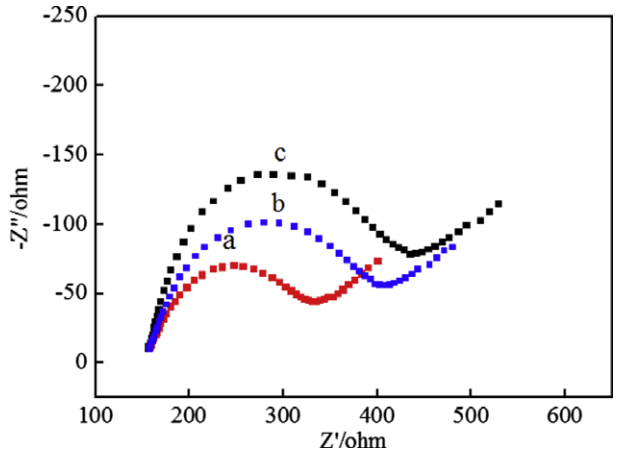

Fig. 7. Electrochemical impedance spectroscopy of modified and unmodified MWCNTs–COOH/GCEs: (a) bare MWCNTs–COOH/GCE; (b) ssDNA/MWCNTs–COOH/GCE; (c) S_1–S_2 hybridized/MWCNTs–COOH/GCE.

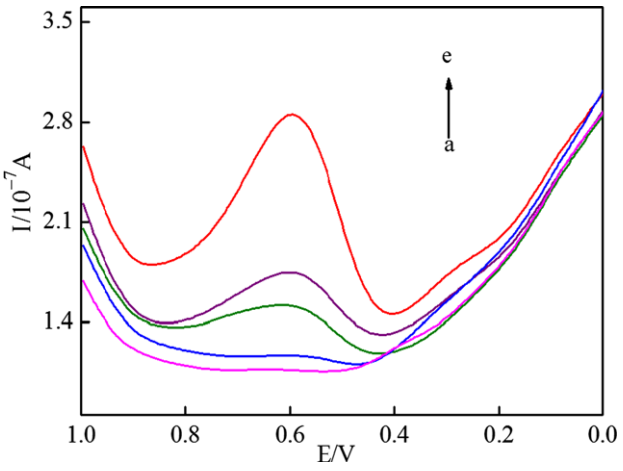

Fig. 8. The DPV curves of different MWCNTs–COOH/GCEs in NaOAc–HOAc buffer solution: (a) S_1/MWCNTs–COOH/GCE; (b) S_1–S_3/MWCNTs–COOH/GCE, where the concentration of S_3 was 6.7 nM; (c) S_1–S_4/MWCNTs–COOH/GCE, where the concentration of S_4 was 4.5 nM; (d) S_1–S_2/MWCNTs–COOH/GCE, where the concentration of S_2 was 4.5 nM; (e) S_1–S_2/MWCNTs–COOH/GCE, where the concentration of S_2 was 11 nM.

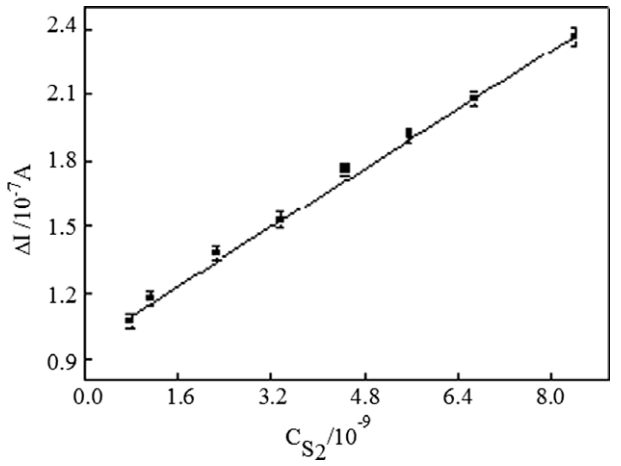

Fig. 9. The increase of the peak current (ΔI) vs. the concentration of complementary target ssDNA (S_2) from 6.7×10^{-10} to 8.4×10^{-9} M in NaOAc–HOAc buffer (pH 6.0).

indicating that only negligible MnL was bound to S_1 on modified MWCNTs–COOH/GCE. A significant increase in the DPV signal was observed after the ssDNA modified MWCNTs–COOH/GCE was hybridized with the complementary ssDNA (S_2). In addition, as expected, there was no significant current difference observed before and after the three-base mismatch sequence (S_3) was applied on ssDNA probe (S_1) modified MWCNTs–COOH/GCE, indicating that the non-specific absorption was negligible. When the concentration of the complementary target (S_2) and single mismatch one (S_4) were of the same, the signal obtained in the case of S_4 was significantly lower than that in the case of S_2, showing that the resulting sensor could distinguish complementary target ssDNA from single mismatched one. A good selectivity was thus obtained for the novel electrochemical DNA biosensor.

3.5. Sensitivities for the detection of target ssDNA

The sensitivity of the prepared DNA electrochemical sensor was investigated using DPV method. The differential peak currents were measured against various concentrations of target ssDNA (Fig. 8). The cathodic peak currents difference was in linear relation with the concentration of target ssDNA in a range from 6.7×10^{-10} M to 8.4×10^{-9} M. The regression equation was found to be $\Delta I_{pc} = 9.46\ \mu A + 1.75(C_{S_2}/10^{-9}\ M)\ \mu A$ with a correlation coefficient of 0.9922. A detection limit of 1.4×10^{-10} M for the target ssDNA was estimated using 3σ (where σ is the standard deviation of the blank solution, $n = 9$).

4. Conclusions

Interaction between MnL and double-stranded salmon sperm dsDNA was studied using CV and fluorescence spectroscopy. It was shown that MnL could be intercalated into double helices of the dsDNA. Functionalized multiwall carbon nanotubes (MWCNTs–COOH) were used for covalent immobilization of ssDNA probe and for the enhancement of sensitivity of sequence-specific ssDNA detection. Using MnL as a novel electroactive indicator, ssDNA fragment could be selectively detected on the novel electrochemical DNA biosensor with a detection limit of 1.4×10^{-10} M and a linear range from 6.7×10^{-10} M to 8.4×10^{-9} M (Fig. 9).

5. Abbreviations

MnL	manganese(II) sodium (*E*)-3-((1-carboxyethylimino) methyl)-4-hydroxy-benzenesulfonate complex
CNT	carbon nanotube
MWCNT	multiwall carbon nanotube
SEM	scanning electron microscope
CV	cyclic voltammetry
DPV	differential pulse voltammetry
EIS	electrochemical impendence spectroscopy
EB	ethidium bromide
PBS	phosphate buffered saline
EDC	1-ethyl-3-(3-dimethylaminopropyl) carbodiimide
GCE	glassy carbon electrode

Acknowledgements

This work was supported by the National Natural Science Foundation of China (No. 20775038), the Scientific and Technical Development Project of Qingdao (06-3-1-4-yx), and the National High-tech R&D Program (863 Program, No. 2007AA09Z113).

References

[1] J. Wang, Anal. Chim. Acta 469 (2002) 63–71.
[2] B. Kuswandi, S. Tombelli, G. Marazza, Chimia 59 (2005) 236–242.
[3] A. Erdem, Talanta 74 (2007) 318–325.
[4] A. Sassolas, B.D. Leca-Bouvier, L.J. Blum, Chem. Rev. 108 (2008) 109–139.
[5] N. Prabhakar, K. Arora, S.P. Singh, H. Singh, B.D. Malhotra, Anal. Biochem. 366 (2007) 71–79.
[6] X.C. Zhou, L.Q. Huang, S.F.Y. Li, Biosens. Bioelectron. 16 (2001) 85–95.
[7] J. Wang, A.N. Kawde, M. Musameh, Analyst 128 (2003) 912–916.
[8] M.L. Pedano, G.A. Rivas, M.L. Pedano, Electrochem. Commun. 6 (2004) 10–16.
[9] A. Erdem, P. Papakonstantinou, H. Murphy, Anal. Chem. 78 (2006) 6656–6659.
[10] J. Wang, G.D. Liu, M.R. Jan, J. Am. Chem. Soc. 126 (2004) 3010–3011.
[11] J. Li, H.T. Ng, A. Cassell, W. Fan, H. Chen, Q. Ye, J. Koehne, J. Han, M. Meyyappan, Nano. Lett. 3 (2003) 597–602.
[12] S.V. Wegner, A. Okesli, P. Chen, C. He, J. Am. Chem. Soc. 129 (2007) 3474–3475.
[13] M.R. Gore, V.A. Szalai, P.A. Ropp, Anal. Chem. 75 (2003) 6586–6592.
[14] Z.W. Zhu, C. Li, N.Q. Li, Microchem. J. 71 (2002) 57–63.
[15] K. Jiao, Q.J. Li, W. Sun, Z.J. Wang, Electroanalysis 17 (2005) 997–1002.
[16] I.T. Ho, G.H. Lee, W.S. Chung, J. Org. Chem. 72 (2007) 2434–2442.
[17] D.H. Johnston, K.C. Glasgow, H.H. Thorp, J. Am. Chem. Soc. 117 (1995) 8933–8938.
[18] T. Lumley-Woodyear, C.N. Campbell, E. Freeman, A. Freeman, G. Georgiou, A. Heller, Anal. Chem. 71 (1999) 535–538.
[19] M.V. del Pozo, C. Alonso, F. Pariente, E. Lorenzo, Anal. Chem. 77 (2005) 2550–2557.

[20] T. Garcia, M. Revenga-Parra, H.D. Abruna, F. Pariente, E. Lorenzo, Anal. Chem. 80 (2008) 77–84.
[21] X.M. Li, H.Q. Ju, C.F. Ding, S.S. Zhang, Anal. Chim. Acta 582 (2007) 158–163.
[22] S.S. Zhang, S.Y. Niu, B. Qu, G.F. Jie, H. Xu, C.F. Ding, J. Inorg. Biochem. 99 (2005) 2340–2347.
[23] S.Y. Niu, S.S. Zhang, L. Wang, X.M. Li, J. Electroanal. Chem. 597 (2006) 111–118.
[24] P.A. Vigato, S. Tamburini, L. Bertolo, Coordin. Chem. Rev. 251 (2007) 1311–1492.
[25] Brian A. Jackson, Jacqueline K. Barton, J. Am. Chem. Soc. 119 (1997) 12986–12987.
[26] Eva Ruba, Jonathan R. Hart, Jacqueline K. Barton, Inorg. Chem. 43 (2004) 4570–4578.
[27] Jens Brunner, Jacqueline K. Barton, Biochemistry 45 (2006) 12295–12302.
[28] Zahid H. Chohan, M. Arif, M. Sarfraz, Appl. Organomet. Chem. 21 (2007) 294–302.
[29] Azadeh Lalehzari, John Desper, Christopher J. Levy, Inorg. Chem. 47 (2008) 1120–1126.
[30] F. Qu, Z. Zhu, N.Q. Li, Electroanalysis 12 (2000) 831–835.
[31] D.W. Pang, H.D. Abruna, Anal. Chem. 70 (1998) 3162–3169.
[32] H.X. Luo, Z.J. Shi, N.Q. Li, Z.N. Gu, Q.K. Zhuang, J. Anal. Chem. 73 (2001) 915–920.